Highly Decorated Lignins in Leaf Tissues of the Canary Island Date Palm *Phoenix canariensis*[1][OPEN]

Steven D. Karlen,[a,b] Rebecca A. Smith,[a,b] Hoon Kim,[a,b] Dharshana Padmakshan,[a,b] Allison Bartuce,[a,b] Justin K. Mobley,[a,b] Heather C. A. Free,[c,d] Bronwen G. Smith,[d] Philip J. Harris,[c] and John Ralph[a,b,2]

[a]Department of Energy Great Lakes Bioenergy Research Center, Wisconsin Energy Institute, University of Wisconsin, Madison, Wisconsin 53726
[b]Department of Biochemistry, University of Wisconsin, Madison, Wisconsin 53706
[c]School of Biological Sciences, University of Auckland, Auckland 1142, New Zealand
[d]School of Chemical Sciences, University of Auckland, Auckland 1142, New Zealand

ORCID IDs: 0000-0002-2044-8895 (S.D.K.); 0000-0003-2363-2820 (R.A.S.); 0000-0001-7425-7464 (H.K.); 0000-0002-2916-0417 (D.P.); 0000-0003-0394-6398 (J.K.M.); 0000-0003-1807-8079 (P.J.H.); 0000-0002-6093-4521 (J.R.).

The cell walls of leaf base tissues of the Canary Island date palm (*Phoenix canariensis*) contain lignins with the most complex compositions described to date. The lignin composition varies by tissue region and is derived from traditional monolignols (ML) along with an unprecedented range of ML conjugates: ML-acetate, ML-benzoate, ML-*p*-hydroxybenzoate, ML-vanillate, ML-*p*-coumarate, and ML-ferulate. The specific functions of such complex lignin compositions are unknown. However, the distribution of the ML conjugates varies depending on the tissue region, indicating that they may play specific roles in the cell walls of these tissues and/or in the plant's defense system.

Lignin is a major component of secondary cell walls of vascular plants and plays a critical role. This difficult-to-break down biopolymer contributes to much of the recalcitrance in the conversion of biomass to liquid fuels and coproducts, prevents pathogens from accessing polysaccharides within cell walls, and, in the walls of xylem tracheary elements, provides a structural framework necessary for transpiration. Lignin polymerizes in the cell wall by stepwise radical coupling of 4-hydroxyphenylpropenoids to a growing copolymer chain. The chemical composition of lignin is dominated by units derived from the monolignols (ML) 4-hydroxycinnamyl (H), coniferyl (G), and sinapyl (S) alcohols but is compatible with a diversity of nontraditional monomers, as reviewed by Vanholme et al. (2012). Examples of nontraditional monomers are caffeyl alcohol, which forms catechyl-lignin that is found in some plant seed coats (Chen et al., 2012), and ferulate (FA), which, in grasses (family Poaceae), chemically links the heteroxylans (glucuronoarabinoxylans) and lignin (Lam et al., 1992; Ralph, 2010).

The chemical composition of lignin often varies with taxon, cell type, and tissue (Harris, 2005). In gymnosperms, most conifers (softwoods) have lignins dominated by G units with small amounts of H units, but under stress generated by tilting the stems, compression wood is formed with lignin that has a much higher proportion of H units (Timmel, 1986; Brennan et al., 2012). Furthermore, in the gnetophyte lineage of gymnosperms, the genera *Gnetum* and *Ephedra* are distinguished in having S/G lignins (Towers and Gibbs, 1953; Melvin and Stewart, 1969). In angiosperms, which include hardwoods (in the eudicotyledons) and grasses (family Poaceae, in the monocotyledons), the lignins have predominately S/G lignins with low levels of H units. Within the angiosperms, there is evidence for differences among cell types. For example, in Arabidopsis (*Arabidopsis thaliana*), the lignins in the walls of xylem tracheary elements are enriched in G units, whereas those in the walls of sclerenchyma fibers are enriched in S units (Schuetz et al., 2013). Even so, this overly simplified view of lignin needed to be modified following the evidence that γ-acylated monolignol conjugates (ML-conj) were building blocks in lignification (Lu and Ralph, 2002, 2008; Lu et al., 2004) and not from post-polymerization modifications.

The addition of ML-conj to the lignin monomer pool added complexity and structural diversity to the portfolio of native lignins. The earliest evidence for acylated lignins was the release of *p*-hydroxycinnamic acids (e.g. *p*-coumarate) from sugarcane (*Saccharum* spp.) lignins

[1] This research was supported by the DOE Great Lakes Bioenergy Research Center (DOE Office of Science BER DE-FC02-07ER64494).

[2] Address correspondence to jralph@wisc.edu.

The author responsible for distribution of materials integral to the findings presented in this article in accordance with the policy described in the Instructions for Authors (www.plantphysiol.org) is: John Ralph (jralph@wisc.edu).

S.D.K., D.P., H.C.A.F., B.G.S., P.J.H., and J.R. designed the research; S.D.K., R.A.S., D.P., A.B., J.K.M., and H.C.A.F. performed the research; S.D.K., R.A.S., H.K., D.P., J.K.M., and J.R. analyzed the data; S.D.K., R.A.S., H.K., J.K.M., B.G.S., P.K.H., and J.R. wrote the article.

[OPEN] Articles can be viewed without a subscription.

www.plantphysiol.org/cgi/doi/10.1104/pp.17.01172

by mild alkaline hydrolysis (Smith, 1955a). Smith (1955b) also showed that *p*-hydroxybenzoate (*p*BA) was linked through ester bonds to the lignin of aspen (*Populus temula*). Although the lignin-ester linkage was identified, it was not until years later that the pathway for their formation was linked to the formation of ML-conj. The first evidence was for monolignol *p*-coumarates (ML-*p*CA), coniferyl and sinapyl *p*-coumarate in bamboo (*Phyllostachys pubesens*) (Nakamura and Higuchi, 1976, 1978), followed by the acetates (Ac), coniferyl acetate and sinapyl acetate in kenaf (*Hibiscus cannabinus*) and poplar (*Populus* spp.; Ralph and Lu, 1998). The ML-Ac conjugates were subsequently shown in kenaf to be formed prior to lignification (Lu and Ralph, 2002, 2008). Much later, the monolignol *p*-hydroxybenzoates (ML-*p*BA) were authenticated as members of the lignin monomer pool (Lu et al., 2015). Most recently, some of the acyltransferase enzymes that form ML-conj were identified and their functions confirmed in planta, particularly for ML-*p*CA (Withers et al., 2012; Bartley et al., 2013; Marita et al., 2014; Petrik et al., 2014; Sibout et al., 2016) and the recently discovered monolignol ferulates (ML-FA; Wilkerson et al., 2014; Karlen et al., 2016).

Palms (family Arecaceae) have long been known to have *p*-hydroxybenzoate, *p*-coumarate, and many other phenolic acids in their leaf-base tissues (Pearl et al., 1959). Despite being known for over 50 years, the function of these wall-bound phenolic acids in the plants remain unknown. However, as some of the phenolic acids are well known preservatives (e.g. sodium benzoate and parabens [which are a family of *p*-hydroxybenzoate esters]), it is believed that the wall-bound phenolic acids play a role in the plant's defense system. Although no evidence was found for any lignin-associated *p*CA in African oil palm (*Elaeis guineensis*) empty fruit bunches (Lu et al., 2015), it was reported to be in leaf-base fiber tissues (Sun et al., 2001). This provided early evidence in palms suggesting organ- and/or tissue-dependent distribution of lignins derived, in part, from ML-conj.

Here, we show that Canary Island date palm (*Phoenix canariensis*) lignification uses an unprecedented range of monolignol conjugates, the distribution of which varies depending on the tissue region, indicating that they may play specific roles in cell walls in these tissues and/or in the plant's defense system.

RESULTS AND DISCUSSION

Thick, transverse segments cut from leaf bases were dissected into inner and outer tissue regions (Fig. 1A). The anatomies of the regions show obvious differences when examined using bright-field light microscopy.

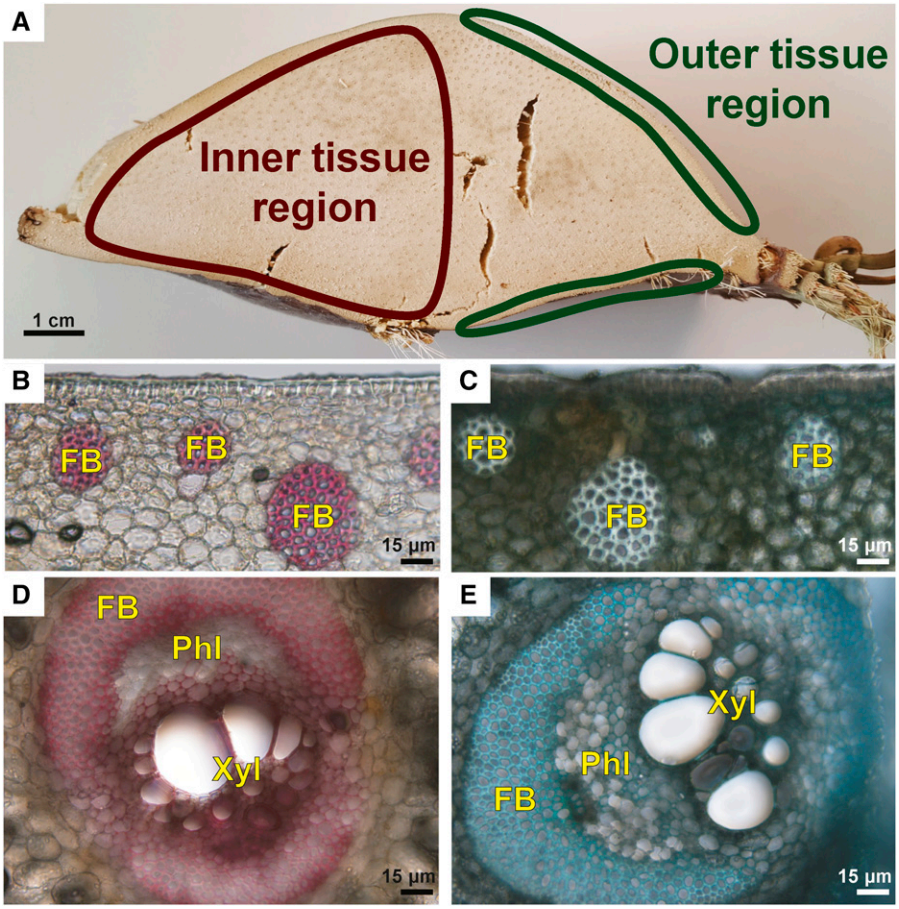

Figure 1. Inner and outer tissue regions of the palm leaf base were sectioned and stained to show the presence of lignified walls. A, A thick, transverse segment of the leaf base used in this study showing the locations of the inner tissue and outer tissue regions. B, Image of a transverse section of the outer tissue region stained with phloroglucinol-HCl showing the red-stained, lignified walls of fibers present in fiber bundles (FB). C, Transverse section of the outer tissue region stained with Toluidine Blue O showing the thick, lignified, blue-stained walls of fibers present in fiber bundles. D, A vascular bundle in the inner tissue region stained with phloroglucinol-HCl. The bundle is surrounded by fibers, and there is a prominent fiber bundle cap over the phloem (Phl); the xylem tissue (Xyl) includes tracheary elements with lignified (red-stained) walls. The walls of the fibers surrounding the vascular bundle, including the cap, show only weak staining with phloroglucinol-HCl. The phloem cell walls were not stained and, therefore, are nonlignified. E, A transverse section of a vascular bundle similar to that in D showing blue staining of the fiber walls and blue-green staining of the tracheary element cell walls with Toluidine Blue O. Bars = 1 cm (A) and 15 μm (B–E).

The outer tissue region consists of an epidermis covered by a waxy cuticle and 20 to 30 layers of parenchyma cells (Fig. 1, B–D). Scattered bundles of fibers are found approximately five parenchyma cell layers below the epidermis. These fibers are defined by their thick secondary cell walls that stain red for lignin with phloroglucinol-HCl (Fig. 1B) and blue with Toluidine Blue O (Fig. 1C), which is consistent with their being lignified. These bundles of fibers provide structural support to the leaf base and to the entire leaf. In the inner tissue region of the leaf base, the scattered fiber bundles are replaced by vascular bundles surrounded by fibers with thick lignified walls, particularly over the adaxially oriented phloem, where they form a cap (Fig. 1, D and E). These fibers also provide mechanical support to the leaf base. The phloem tissue has thin primary cell walls that do not stain with phloroglucinol-HCl (Fig. 1D) but stain very dark purple-blue with Toluidine Blue O, consistent with their being nonlignified (Fig. 1E). Located abaxially are the water-conducting xylem tracheary elements with lignified secondary cell walls. The vascular bundles are embedded in parenchyma tissue (Fig. 1, D and E). The differences between the outer and inner tissue regions could have implications for the lignin content and the lignin composition for the different parts of the leaf base.

Mild alkaline hydrolysis of cell walls from the outer tissue region released over 10 times the amount of *p*CA and almost twice as much FA as from the cell walls from the inner tissue region (Table I). In contrast, hydrolysis of cell walls from the inner tissue region released over 5 times as much benzoate (BA) and almost 1.5 times the amount of *p*BA as the outer tissue region. Other minor components also were released; however, these were not identified or quantified.

Pearl et al. (1959) showed, in an extensive survey of 26 palm species that included representatives of three of the five subfamilies now recognized (Asmussen et al., 2006), that alkaline hydrolysis of all of palm petioles released a variety of phenolic acids, including *p*BA, vanillic acid (VA), and syringic acid. Although the extraction and quantification techniques differed slightly, our mild alkaline hydrolysis data and the reported data of Pearl et al. (1959) indicated similar amounts of base-labile *p*BA and FA.

These differences in lignin decoration between the two tissue regions also were quite dramatically revealed by 2D heteronuclear single-quantum coherence (HSQC) NMR spectroscopy (Lu and Ralph, 2003; Wagner et al., 2007; Kim and Ralph, 2010; Mansfield et al., 2012), performed in dimethyl sulfoxide (DMSO)-d_6/pyridine-d_5 on lignins that had been treated with crude cellulases to remove the polysaccharides (Chang et al., 1975; Wagner et al., 2007). The HSQC spectra of the outer tissue region showed the presence of *p*BA and *p*CA (Fig. 2A), whereas the inner tissue region had signals corresponding to *p*BA and a new component that corresponds to BA (Fig. 2B). To our knowledge, this is the first lignin sample that we are aware of with strong HSQC correlation signals for BA. This correlation signal has not been observed for plants from other families within the commelinid monocotyledons, such as the grass family Poaceae (e.g. *Zea mays*, *Oryza sativa*, and *Brachypodium distachyon*), for which many wild-type and transgenic lines have been characterized by 2D HSQC NMR (Kim and Ralph, 2010; del Río et al., 2012; Petrik et al., 2014). Nor has the BA been associated with the noncommelinid monocotyledon family Asparagaceae (e.g. *Agave sisalana*); therefore, the presence of wall-bound benzoates (BA, *p*BA, and VA) seems to be a trait that developed within the palms (Arecaceae).

The lignin composition of the cell walls in the two tissue regions was determined by derivatization followed by reductive cleavage (DFRC; Lu and Ralph, 1997). In this assay, the β-ether bonds in the lignin structure are cleaved while leaving the γ-ester-linked subunits intact, generating diagnostic products for

Table I. *Analytical data on cell walls from the two tissue regions*

Mp, Peak average M_r values; WCW, whole cell wall material. Other abbreviations are given in the text.

Parameter	Inner Tissue Region	Outer Tissue Region
Klason lignin (wt% WCW)		
Total lignin	20.98 ± 0.25	24.20 ± 0.70
Insoluble lignin	16.76 ± 0.17	20.41 ± 0.89
Soluble lignin	4.23 ± 0.18	3.79 ± 0.24
Saponification (wt% WCW)		
Benzoic acid	0.47 ± 0.05	0.08 ± 0.01
p-Hydroxybenzoic acid	12.08 ± 0.53	8.17 ± 0.65
p-Coumaric acid	0.16 ± 0.09	1.68 ± 0.20
Ferulic acid	0.19 ± 0.07	0.35 ± 0.08
Enzyme lignin		
Mw (kD)	15.0	8.2
Mn (kD)	2.1	1.8
Mp (kD)	8.7	7.6
Mw/Mn	7.1	4.6
dn/dc (mL g^{-1})	0.0669 ± 0.0028	0.0637 ± 0.0043
ε [λ = 280 nm] (mL mg^{-1} cm^{-1})	8.818 ± 0.005	11.536 ± 0.038

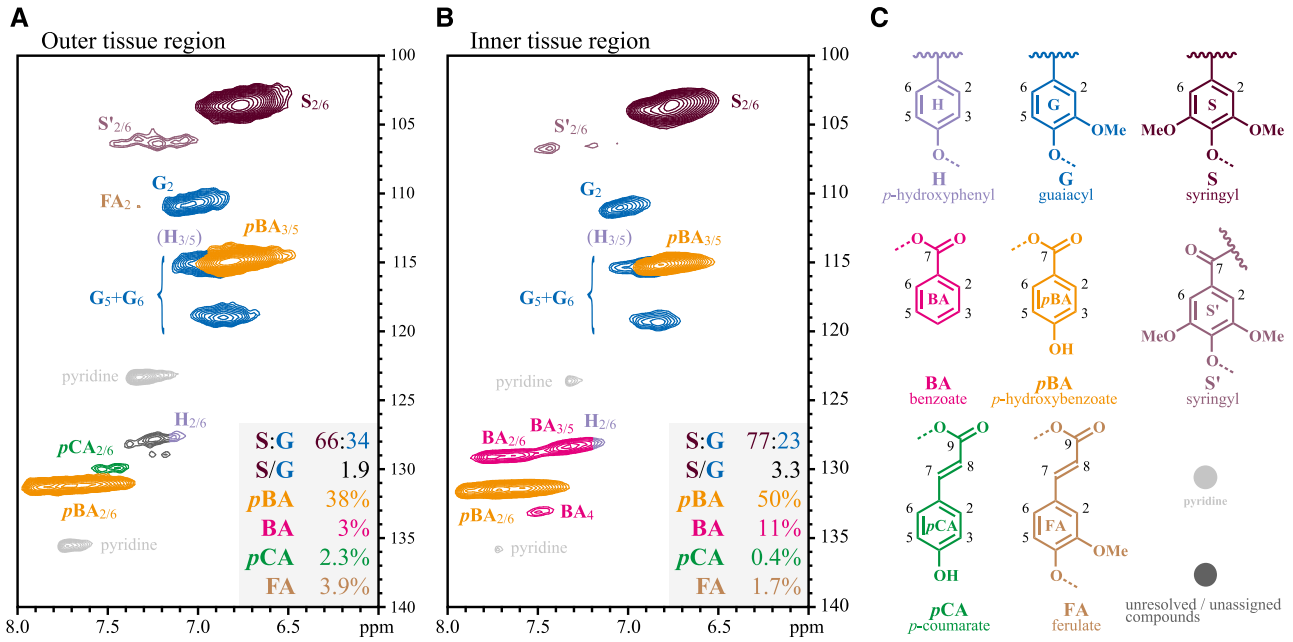

Figure 2. 2D HSQC NMR spectra of enzyme lignins (EL) of leaf base tissue. A, Outer tissue region. B, Inner tissue region. C, Cell wall components detected by HSQC NMR. The *p*CA, along with traces of FA, are present in the outer tissue region, whereas BA is visible only in the inner tissue region, and *p*BA is found throughout the leaf base. Tabulated values are from contour volume integrals only and are on an S + G = 100 basis. Note that the mobile end groups on the polymer (including BA, *p*BA, *p*CA, and FA) have integrals that overrepresent their concentrations relative to internal units in these spectra (Mansfield et al., 2012).

ML conjugates. Distributions of the normal monolignols (with a γ-OH, ML-OH), versus conjugates ML-Ac and the others, can be estimated using a combination of DFRC and a modification of this method, DFRC-Pr, in which the acetic acid, acetyl bromide, and acetic anhydride are replaced with their propionate analogs (Ralph and Lu, 1998). Using the standard DFRC assay, in which the acetylation of hydroxyls occurs, the ML-Ac conjugates become quantified as part of the normal γ-OH units (ML-OH) to yield a compositional ratio of ML (in this case, ML-OH + ML-Ac) to the other ML-conj. The DFRC-Pr reaction conditions allow the ratio of natural ML-OH to ML-Ac to be quantified. Combined, the two methods provide a complete breakdown of the various ML-OH-to-ML-conj ratios (Fig. 3).

The DFRC assay confirmed that, in the leaf-base samples, the lignins were decorated with at least six different classes of conjugates: ML-Ac, ML-BA, ML-*p*BA, ML-VA, ML-*p*CA, and ML-FA (Fig. 3; Table II), differing in their relative ratios depending on the region. The inner tissue region lignins had significantly higher levels of BA as well as *p*BA, whereas the outer tissues had much higher levels of *p*CA, in agreement with the NMR data.

The DFRC-Pr results showed that the lignins from both tissue regions contained natural ML-Ac (Fig. 3; Table II). The inner tissue region released monolignols that were found to have γ-acetates on 18% of the G units, 63% of the S units, and a negligible proportion of the H units (Table II). The outer tissue region released monolignols that were found to have γ-acetates on 22% of the G units, 63% of the S units, and a negligible proportion of the H units.

Applying the ML-OH-to-ML-Ac ratio determined by DFRC-Pr to the ML products quantified by DFRC teases apart how much of the total quantified DFRC products was initially γ-esters (ML-conj) and what fraction was actually free γ-hydroxyl (ML-OH). The outer tissue region was composed of 37% ML-OH and 63% ML-conj, of which 58% was ML-Ac, whereas the inner tissue region was 33% ML-OH and 67% ML-conj, of which 51% was ML-Ac. In both cases, the majority of the ML conjugates was sinapyl acetate (S-Ac) and sinapyl *p*-hydroxybenzoate (S-*p*BA). There were only trace amounts of ML-VA and ML-FA released from all the tissues, but, as we noted previously (Wilkerson et al., 2014), the ferulates and, analogously, the vanillates have low DFRC release efficiency.

The relative M_r values of the enzyme lignins isolated from the inner and outer leaf-base tissue regions were determined by size-exclusion chromatography (SEC) using a conventional calibration curve created with polystyrene standards and synthetic lignin model compounds with similar hydrodynamic volumes to dimers, trimers, and tetramers (Fig. 4). In order to be consistent, the M_r determinations were made from 36.5 to 57 min, the point at which the signal returned to the baseline. The samples, analyzed in dimethylformamide (DMF) with 0.1 M lithium bromide, were found to have weight-average M_r values (Mw) of 8.2 kD for the outer tissue region and 15 kD for the inner tissue region. The Mw of the lignin from the outer tissue region was similar to the 7.9 kD reported for coconut (*Cocos nucifera*) coir fiber (Rencoret et al., 2013) and much lower

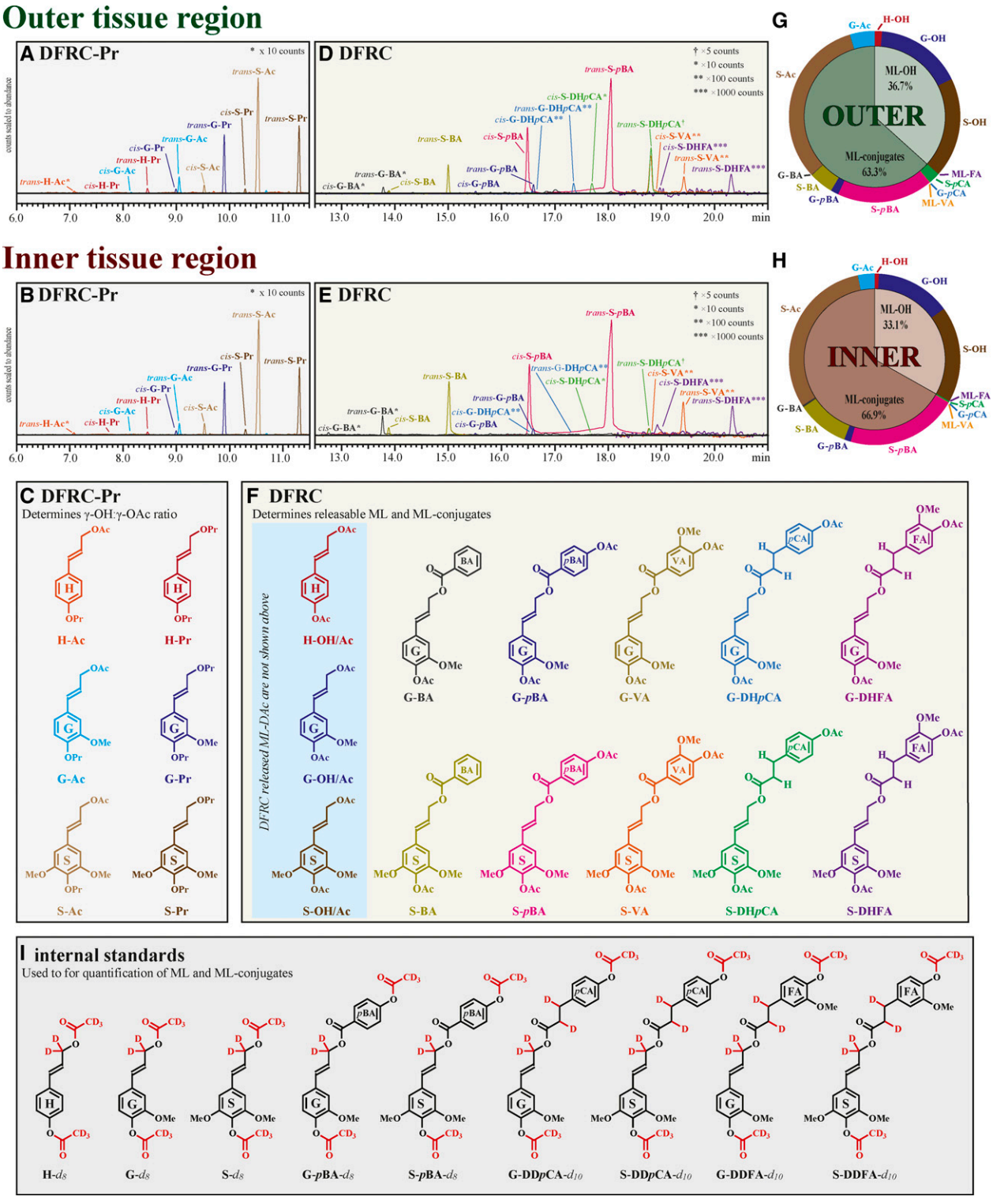

Figure 3. DFRC and DFRC-Pr of the leaf base tissue regions reveal the compositional complexity and tissue region specificity of the lignin composition. The DFRC-Pr multiple reaction monitoring (MRM) chromatograms of the outer (A) and inner (B) tissue regions elucidated the ratio of γ-hydroxyl (ML-Pr) to γ-acetate (ML-Ac) on the monolignols (C). The DFRC MRM-chromatograms (D and E) show the compositional complexity of the leaf base lignins (F). The signal intensities in these composite chromatograms have been scaled to be representative of abundances, with low-level components scaled to ×5 (†), ×10 (*), ×100 (**), and ×1,000 (***) counts. The pie charts (G and H) provide a visual of the distribution of the ML and ML-conj released by DFRC/DFRC-Pr. The detected products from DFRC-Pr (C), DFRC (F), and the internal standards (I) are shown with their respective abbreviations.

Table II. *Lignin components released from cell walls from the two tissue regions and quantified by DFRC and DFRC-Pr*

Masses were converted to the native M_r values and not the acetylated/hydrogenated M_r values detected by gas chromatography (GC)-MRM-mass spectrometry (MS). All values are reported here as mg g^{-1} EL (μmol g^{-1} EL) ± SE. N/D, Not detected; –, not applicable.

Component	DFRC		DFRC-Pr		Applying ML-OH-to-ML-Ac Ratio to the DFRC Results	
	Outer Tissue	Inner Tissue	Outer Tissue	Inner Tissue	Outer Tissue	Inner Tissue
H-OH/Ac[a]	2.4 ± 0.1[a] (10.1 ± 0.5)	1.9 ± 0.1[a] (8.1 ± 0.2)	–	–	–	–
G-OH/Ac[a]	39.6 ± 1.0[a] (150 ± 4)	45.4 ± 4.5[a] (172 ± 17)	–	–	–	–
S-OH/Ac[a]	107 ± 3[a] (365 ± 9)	143 ± 5[a] (487 ± 16)	–	–	–	–
H-OH[b]	–	–	1.0 ± 0.1 (6.8 ± 0.9)	1.0 ± 0.0 (6.4 ± 0.2)	1.5 ± 0.1 (10.1 ± 0.5)	1.2 ± 0.0 (8.1 ± 0.2)
G-OH[b]	–	–	14.3 ± 0.2 (79.6 ± 1.2)	12.9 ± 0.3 (71.8 ± 1.9)	21.1 ± 0.5 (117 ± 3)	25.4 ± 2.5 (141 ± 14)
S-OH[b]	–	–	18.2 ± 0.3 (86.6 ± 1.3)	17.0 ± 2.1 (80.9 ± 10)	28.4 ± 0.7 (135 ± 3)	37.9 ± 1.3 (180 ± 6)
H-Ac[c]	–	–	–	–	–	–
G-Ac[c]	–	–	5.1 ± 1.5 (23.1 ± 6.6)	3.5 ± 0.0 (15.6 ± 0.1)	7.3 ± 0.2 (33 ± 1)	6.9 ± 0.7 (31 ± 3)
S-Ac[c]	–	–	38.9 ± 6.1 (154 ± 24)	34.1 ± 2.1 (135 ± 8)	58.0 ± 1.5 (230 ± 6)	77.3 ± 2.6 (307 ± 10)
G-BA	0.2 ± 0.0 (0.8 ± 0.1)	1.0 ± 0.1 (3.6 ± 0.3)	–	–	0.2 ± 0.0 (0.8 ± 0.1)	1.0 ± 0.1 (3.6 ± 0.3)
S-BA	10.2 ± 0.3 (33 ± 1)	30.7 ± 4.4 (98 ± 14)	–	–	10.2 ± 0.3 (33 ± 1)	30.7 ± 4.4 (98 ± 14)
G-*p*BA	3.2 ± 0.2 (10.6 ± 0.8)	3.7 ± 0.2 (12.5 ± 0.7)	–	–	3.2 ± 0.2 (10.6 ± 0.8)	3.7 ± 0.2 (12.5 ± 0.7)
S-*p*BA	42.7 ± 3.4 (129 ± 10)	69.1 ± 1.2 (209 ± 3)	–	–	42.7 ± 3.4 (129 ± 10)	69.1 ± 1.2 (209 ± 3)
G-VA	0.01 ± 0.00 (0.02 ± 0.00)	0.01 ± 0.00 (0.03 ± 0.00)	–	–	0.01 ± 0.00 (0.02 ± 0.00)	0.01 ± 0.00 (0.03 ± 0.00)
S-VA	0.15 ± 0.01 (0.40 ± 0.03)	0.22 ± 0.01 (0.62 ± 0.04)	–	–	0.15 ± 0.01 (0.40 ± 0.03)	0.22 ± 0.01 (0.62 ± 0.04)
G-*p*CA	0.04 ± 0.00 (0.12 ± 0.00)	0.01 ± 0.00 (0.02 ± 0.00)	–	–	0.04 ± 0.00 (0.12 ± 0.00)	0.01 ± 0.00 (0.02 ± 0.00)
S-*p*CA	5.53 ± 0.01 (15.5 ± 0.0)	0.86 ± 0.01 (2.4 ± 0.0)	–	–	5.53 ± 0.01 (15.5 ± 0.0)	0.86 ± 0.01 (2.4 ± 0.0)
G-FA	N/D	N/D	–	–	N/D	N/D
S-FA	0.01 ± 0.00 (0.02 ± 0.00)	0.02 ± 0.00 (0.05 ± 0.01)	–	–	0.01 ± 0.00 (0.02 ± 0.00)	0.02 ± 0.00 (0.05 ± 0.01)

[a]Released by DFRC and reported here as the monolignol 4,9-diacetate. [b]Released by DFRC-Pr as the monolignol 4,9-dipropionate; reported as the 4,9-dihydroxy-monolignol. [c]Released by DFRC-Pr as the monolignol 4-propionate-9-acetate; reported as the 4-hydroxy-monolignol 9-acetate.

than that reported for hemicellulose-rich enzyme lignin (~23 kD) obtained from oil palm trunk (Sun et al., 1998). It should be noted, however, that M_r and lignin structure are known to be altered by lignin isolation methods, including by the mechanical forces experienced in ball milling (Chang et al., 1975). Thus, comparing the M_r of lignins from different tissues should be performed using samples prepared under the same conditions.

Although there is a large difference in overall Mw between the lignins from the inner and outer tissue regions, closer inspection of the M_r distributions shows that the lignin polymers are actually much closer in size than appears from Mw. The number-average M_r (Mn) for the lignin from the inner tissue region is 2.1 kD, compared with 1.8 kD for that from the outer tissue region. The peak average M_r values of the lignin from the inner and outer tissue regions were also fairly similar: 8.7 kD for the inner tissue region compared with 7.6 kD for the outer tissue region. Moreover, comparison of the polydispersity of the two lignins shows that the lignin from the inner tissue region (Mw/Mn = 7.1) has a lot more variability in M_r than that from the outer tissue region (Mw/Mn = 4.6).

The observed higher M_r of the lignins in the inner tissue region could be due to larger polymer chains and/or a higher compositional percentage of large-chain polysaccharides. The lower extinction coefficient (ε; λ = 280 nm) and higher specific refractive index (dn/dc; λ = white light) measured for the inner tissue region lignin suggest that it has fewer monolignols and *p*-hydroxycinnamates (which absorb 280-nm light) than the lignin isolated from the outer tissue region. This analysis is complicated by the differences in lignin composition and because *p*BA, BA, waxes (present on the outer tissues; Fig. 1), and polysaccharides all do not efficiently absorb 280-nm radiation. The inner and outer tissue regions do have different cell type distributions (e.g. tracheary elements versus fibers), and the outer tissue region experiences very different environmental conditions (i.e. exposure to sunlight, oxidation, and weathering). These biological and environmental factors are likely responsible for producing the observed larger lignin polymer chains in the inner tissue region rather than differences in lignin/polysaccharide compositions.

CONCLUSION

The lignins in the cell walls of the leaf-base tissue regions from the Canary Island date palm have some of the most complex compositions reported to date. They derive from the traditional H, G, and S monolignols (i.e. from *p*-coumaryl alcohol, coniferyl alcohol, and sinapyl alcohol, respectively) and an array of ML-conj (ML-Ac, ML-BA, ML-*p*BA, ML-*p*CA, ML-VA, and ML-FA). These ML conjugates are not evenly distributed throughout the tissue regions of the leaf base but show some tissue region specificity. Most notable are the higher levels of ML-*p*CA in lignins from the outer tissue region and ML-BA in lignins from the inner tissue region. Unfortunately, we were unable to isolate the individual cell types to further resolve which cell walls were predominantly expressing ML-*p*CA versus ML-BA.

To our knowledge, this is the first plant species that has been shown to contain ML-BA and ML-VA incorporated into its lignin. The presence of ML-BA and ML-VA suggests either some flexibility in monolignol acyltransferase selectivity or the presence of benzoyl-CoA monolignol transferases with different chemical specificity; the latter is more likely, as the ML-BA was located predominantly in the inner tissue region. The discovery of ML-BA and ML-VA incorporation into lignin further expands the growing list of carboxylic acids known to acylate monolignols via their γ-hydroxyl groups and that have been confirmed in planta to participate in cell wall lignification. The presence of so many different ML conjugates further demonstrates the plasticity of lignification, the diversity of lignin subunits, and the chemical complexity of the lignin polymer.

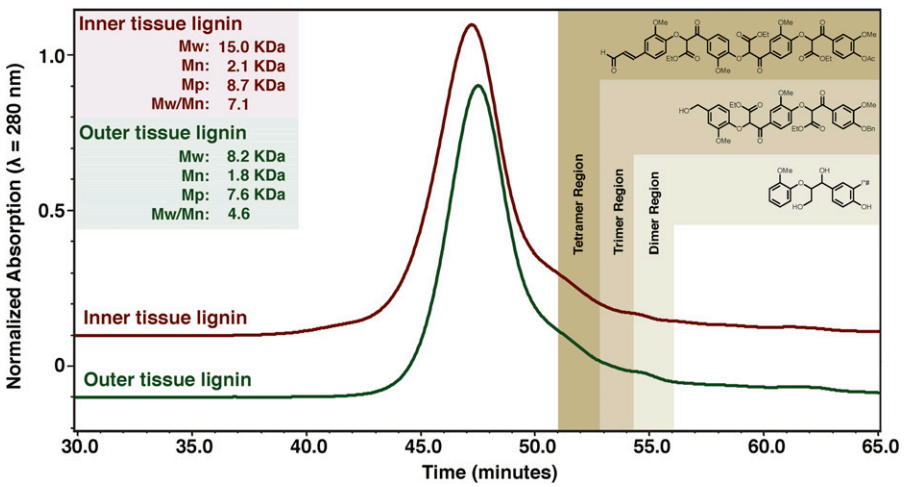

Figure 4. SEC analysis of leaf base lignins isolated from ball-milled tissue regions using cellulase digestion. SEC analysis is shown for outer (dark green) and inner (burgundy) tissue regions (as in Figure 1). M_r regions of lignin oligomers were determined using authentic standards. M_r values of the dimer, trimer, and tetramer shown are 320, 716, and 928 g mol^{-1}.

MATERIALS AND METHODS

General

Commercial chemicals, including solvents, were of reagent grade or better and used without further purification. GC-MRM-MS was performed on a Shimadzu GCMS-TQ8030 instrument, with the acquisition parameters described in Supplemental Tables S1 and S2.

Plant Materials

The bases of the leaf petioles were collected from two mature Canary Island date palms (*Phoenix canariensis* 'Chabaud') growing at two sites (Madden Street and Stokes Road in Auckland, New Zealand).

Microscopy

A small piece (~2 cm^3) was cut from a thick (~15 × 6.5 × 5.5 cm) transverse segment from the base of a petiole. The small piece, containing both outer and inner tissue regions (Fig. 1A), was dissected into these regions and soaked in water for 24 h. Thin transverse sections of the outer and inner tissue regions were cut by hand with a double-edged razor blade and stained prior to imaging. Sections were stained with an aqueous solution of Toluidine Blue O (0.5%, w/v) for less than 1 min and mounted in water. Sections also were stained for 5 min with a phloroglucinol-HCl solution (10% [w/v] phloroglucinol in 95% [v/v] ethanol with five drops of 1 M HCl). The sections were mounted in the staining solution and examined by bright-field light microscopy using an Olympus BX60 epifluorescence microscope with 10×, 20×, and 40× objective lenses. Images were obtained using a DP73 color camera and CellSens software (Olympus America).

Sample Preparation and Lignin Isolation

WCW samples were prepared by the following procedure. The thick (~15 × 6.5 × 5.5 cm) transverse segments of leaf bases, after air drying at 50°C, were divided into outer and inner tissue regions (as indicated in Fig. 1A) and shaker milled to a fine powder (Retsch MM400). This was then solvent extracted sequentially with water (3 × 45 mL), 80% ethanol (3 × 45 mL), and acetone (1 × 45 mL) by first suspending the sample in solvent, sonicating for 20 min, pelleting by centrifuging (8,800*g* for 20 min; Sorvall Biofuge Primo centrifuge), and discarding the supernatant. The extract-free pellet was then dried under vacuum and submitted to chemical analysis.

ELs were prepared from ball-milled cell wall materials as described previously (Chang et al., 1975; Wagner et al., 2007). Briefly, extract-free WCWs were ball milled with a Fritsch pulverisette 7 (1 g, 30-mL ZrO_2 jar, 10- × 10-mm ZrO_2 balls, 600 rpm for 10 min, 5-min rest, 46 cycles, reverse on). The ball-milled powder (1 g) was transferred to 50-mL centrifuge tubes, suspended in 40 mL of 50 mM sodium acetate buffer (pH 5), and treated with crude cellulases (40 mg; Cellulysin; EMD Biosciences). The samples were incubated at 35°C on a shaker table shaking at 225 rpm for 3 d. After incubation, solids were pelleted by centrifugation (8,800*g* for 20 min; Sorvall Biofuge Primo centrifuge), and the supernatant was decanted. The pelleted solids were then treated a second time with fresh crude cellulases (40 mg) for 3 d, pelleted, and washed with reverse osmosis water (3 × 40 mL). The washed, pelleted solids were dried on a freeze dryer to yield ~10% of the dry weight of the original ball-milled cell wall material, presumably containing all of the lignin but also low levels of residual polysaccharides.

NMR Analysis

The EL samples were prepared in NMR tubes (20 mg for each sample) and dissolved using DMSO-d_6/pyridine-d_5 100% (4:1, v/v, 500 μL; Kim et al., 2008; Kim and Ralph, 2010). NMR spectra were acquired on a Bruker Biospin AVANCE-III 700-MHz spectrometer equipped with a 5-mm quadruple-resonance $^1H/^{31}P/^{13}C/^{15}N$ QCI gradient cryoprobe with inverse geometry (proton coils closest to the sample). The central DMSO solvent peak was used as an internal reference (δ_C 39.5, δ_H 2.49 ppm). The ^1H-^{13}C correlation experiment was an adiabatic HSQC experiment (Bruker standard pulse sequence hsqcetgpsisp2.2; phase-sensitive gradient-edited 2D HSQC using adiabatic pulses for inversion and refocusing). HSQC experiments were carried out using the following parameters: acquired from 10 to 0 ppm in F2 (^1H) with 2,800 data points (acquisition time, 200 ms), 200 to 0 ppm in F1 (^{13}C) with 560 increments (F1 acquisition time, 8 ms) of 32 scans with a 1-s interscan delay; the d_{24} delay was set to 0.86 ms (1/8J, J = 145 Hz). The total acquisition time for a sample was 6 h. Processing used typical matched Gaussian apodization (Gaussian broadening factor, GB = 0.001, exponential line-broadening factor, LB = −0.1) in F2 and squared cosine-bell and one level of linear prediction (32 coefficients) in F1. The volume integration of contours in HSQC plots used Bruker's TopSpin 3.5pl6 (Mac version) software. NMR analysis was performed on two ELs from two biological samples of leaf bases and two technical replicates.

Mild Alkaline Hydrolysis

The determination of ester-linked carboxylic acids was performed on extract-free WCW using mild alkaline hydrolysis (2 M NaOH, 20 h at room temperature) following previously published procedures (Ralph et al., 1994).

Klason Lignin Analysis

Acid-insoluble lignin was determined using Klason lignin analysis as described previously (Coleman et al., 2008). The analysis was performed on 150 to 200 mg of extractive-free WCW. Acid-soluble lignin was determined by measuring the absorbance of the filtrate after the isolation of acid-insoluble lignin at 205 nm and calculated using an ε of 110 L g^{-1} cm^{-1}.

DFRC Procedure

Incorporation of ML-conj into the lignin was determined using the ether-cleaving ester-retaining DFRC method established previously for ML-*p*CA, ML-FA, and ML-*p*BA conjugates (Lu and Ralph, 1999, 2014; Petrik et al., 2014; Wilkerson et al., 2014; Lu et al., 2015). The DFRC protocol used here was as follows.

EL samples (35−50 mg) were stirred in 2-dram vials fitted with polytetrafluoroethylene pressure-release caps in acetyl bromide:acetic acid (1:4, v/v, 4 mL). After heating for 3 h at 50°C, the solvents were removed on a SpeedVac (Thermo Scientific SPD131DDA; 50°C, 35 min, 1 torr, 35 torr min^{-1}). Crude films were suspended in absolute ethanol (0.5 mL), dried on the SpeedVac (50°C, 15 min, 6 torr, 35 torr min^{-1}), and then suspended in dioxane:acetic acid:water (5:4:1, v/v/v, 5 mL) with nano-powdered zinc (250 mg). The vials were then sealed, sonicated to ensure the suspension of solids, and stirred in the dark at room temperature for 16 to 20 h. The reaction mixtures were then quantitatively transferred with dichloromethane (DCM; 6 mL) into separatory funnels charged with saturated ammonium chloride (10 mL) and the isotopically labeled internal standards. Organics were extracted with DCM (4 × 10 mL), combined, dried over anhydrous sodium sulfate, and filtered, and the solvents were removed via rotary evaporation (water bath at less than 50°C). Free hydroxyl groups on DFRC products were then acetylated for 16 h in the dark using a solution of pyridine and acetic anhydride (1:1, v/v, 5 mL), after which the solvents were removed on a rotary evaporator to yield crude oily films. To remove most of the polysaccharide-derived products, acetylated DFRC products were loaded onto SPE cartridges (3-mL Supelco Supelclean LC-Si SPE tube; P/N: 505048) with DCM (2 × 1 mL). After elution with hexanes:ethyl acetate (1:1, v/v, 8 mL), the eluted organics were combined and the solvents were removed by rotary evaporation. The products were transferred in stages with GC-MS-grade DCM to GC-MS vials containing a 300-μL insert, with the final sample volumes of 200 μL. Samples were analyzed on a triple-quadrupole GC/MS/MS device (Shimadzu GCMS-TQ8030) operating in MRM mode using synthetic standards (for the synthesis of the new standard compounds ML-BA and ML-VA, see Supplemental Fig. S1) and isotopically labeled internal standards (Fig. 3I) for authentication. The GC program and acquisition parameters are listed in Supplemental Table S1, and the results of the DFRC assay are listed in Table II and Figure 3.

DFRC-Pr Procedure

The DFRC-Pr procedure was developed to determine the ratio of ML-Ac to ML-OH (Ralph and Lu, 1998). The procedure is analogous to that of DFRC, using propionic acid, propionyl bromide, and propionic anhydride in place of the acetic acid, acetyl bromide, and acetic anhydride.

Lignin M_r Profiles

The relative M_r values of lignins isolated from inner and outer tissue regions were determined by SEC utilizing a Shimadzu LC20-AD LC pump equipped

with a Shimadzu SPD-M20A UV-Vis detector set at 280 nm and a series of TOSOH Biosciences GPC columns (TSKgel Guard Alpha-M, 6 mm i.d. × 4 cm, 13 μm; TSKgel Alpha-M, 7.8 mm i.d. × 30 cm, 13 μm; TSKgel Alpha-2500, 7.8 mm i.d. × 30 cm, 7 μm). The samples (SIL-20AC HT autoinjector) and column compartment (Shimadzu CTO-20A) were held at 40°C during analysis. The mobile phase for SEC was DMF with 0.1 M lithium bromide to solubilize and effectively disperse the lignins, ideally with minimal to no aggregation of the polymer chains. This allows for the separation of the components by hydrodynamic volume. M_r distributions were determined via a conventional calibration curve using a ReadyCal Kit from Sigma-Aldrich ([76552, M(p) 250-70000] and Wyatt ASTRA 7 software. The samples were prepared at ~1 mg mL^{-1}.

Lignin Hydrodynamic Volume Model Compounds

Three lignin model compounds were synthesized to function as GPC standards for monolignol oligomers. The classic G-G β-*O*-4 model compound guaiacylglycerol-β-guaiacyl ether (Lundquist and Remmerth, 1975), lignin dimer in Figure 4, was selected to represent compounds of similar hydrodynamic volume as a compound formed from the radical coupling of two monolignols. The G-G model compound was prepared following the synthesis described previously (Lu et al., 2015). Larger hydrodynamic volume representatives, lignin tetramer, lignin trimer, and lignin dimer structures in Figure 4, were chosen based on their ease of synthesis and such that they most closely represent linear β-ether chains. The two compounds were synthesized by stepwise condensation of acetovanillone to form β-linked diketo ester (Supplemental Figs. S2 and S3) under reaction conditions similar to those reported by Kishimoto et al. (2008a, 2008b).

Lignin dn/dc Determination

The dn/dc was determined using a Shimadzu LC20AD pump equipped with a 2-mL manual injection loop and a Shimadzu RID-10A detector, along with Wyatt ASTRA 7 software. The eluent was 0.1 M LiBr in DMF. The samples were prepared via serial dilution at ~1 mg mL^{-1}; however, exact concentrations were determined via the differential weight of the filter membranes (in series, polytetrafluoroethylene 1 and 0.2 μm, respectively) after washing the membrane with 80% ethanol/water and acetone (~20 mL each) to remove residual LiBr and DMF. Lignin samples were injected at 0.0128, 0.0257, 0.0514, 0.1028, 0.2055, and 0.4110 mg mL^{-1} from the outer tissue region and 0.0385, 0.0770, 0.1540, 0.3080, 0.6160, and 1.2320 mg mL^{-1} from the inner tissue region. Error is reported as given by ASTRA 7 software.

Extinction coefficient (ε)

The ε at 280 nm was determined using a Shimadzu UV-1800 UV spectrophotometer operated with Shimadzu UVProbe 2.43 software. Samples were analyzed at concentrations of 0.0128, 0.0257, and 0.0514 mg mL^{-1} for the outer tissue region and 0.0385 and 0.0770 mg mL^{-1} for the inner tissue region. Errors are reported as SE.

Supplemental Data

The following supplemental materials are available.

Supplemental Figure S1. Synthesis of G-B, S-B, G-V, and S-V reference compounds.

Supplemental Figure S2. Synthesis of monolignol trimer.

Supplemental Figure S3. Synthesis of monolignol tetramer.

Supplemental Table S1. Chromatography program for GC-MS/MS characterization of the DFRC product mix.

Supplemental Table S2. MRM parameters for GC-MS/MS characterization of the DFRC and DFRC-Pr product mixes.

ACKNOWLEDGMENTS

The bright-field microscopy was performed at the Newcomb Imaging Center, Department of Botany, University of Wisconsin, Madison.

Received August 22, 2017; accepted September 6, 2017; published September 11, 2017.

LITERATURE CITED

Asmussen CB, Dransfield J, Deickmann V, Barfod AS, Pintaud JC, Baker WJ (2006) A new subfamily classification of the palm family (Arecaceae): evidence from plastid DNA phylogeny. Bot J Linn Soc **151:** 15–38

Bartley LE, Peck ML, Kim SR, Ebert B, Manisseri C, Chiniquy DM, Sykes R, Gao L, Rautengarten C, Vega-Sanchez ME, et al (2013) Overexpression of a BAHD acyltransferase, OsAt10, alters rice cell wall hydroxycinnamic acid content and saccharification. Plant Physiol **161:** 1615–1633

Brennan M, McLean JP, Altaner C, Ralph J, Harris PJ (2012) Cellulose microfibril angles and cell-wall polymers in different wood types of *Pinus radiata*. Cellulose **19:** 1385–1404

Chang HM, Cowling EB, Brown W, Adler E, Miksche G (1975) Comparative studies on cellulolytic enzyme lignin and milled wood lignin of sweetgum and spruce. Holzforschung **29:** 153–159

Chen F, Tobimatsu Y, Havkin-Frenkel D, Dixon RA, Ralph J (2012) A polymer of caffeyl alcohol in plant seeds. Proc Natl Acad Sci USA **109:** 1772–1777

Coleman HD, Park JY, Nair R, Chapple C, Mansfield SD (2008) RNAi-mediated suppression of *p*-coumaroyl-CoA 3′-hydroxylase in hybrid poplar impacts lignin deposition and soluble secondary metabolism. Proc Natl Acad Sci USA **105:** 4501–4506

del Río JC, Rencoret J, Prinsen P, Martínez ÁT, Ralph J, Gutiérrez A (2012) Structural characterization of wheat straw lignin as revealed by analytical pyrolysis, 2D-NMR, and reductive cleavage methods. J Agric Food Chem **60:** 5922–5935

Harris PJ (2005) Diversity in plant cell walls. *In* RJ Henry, ed, Plant Diversity and Evolution: Genotypic and Phenotypic Variation in Higher Plants. CABI International, Wallingford, UK, pp 201–228

Karlen SD, Zhang C, Peck ML, Smith RA, Padmakshan D, Helmich KE, Free HCA, Lee S, Smith BG, Lu F, et al (2016) Monolignol ferulate conjugates are naturally incorporated into plant lignins. Sci Adv **2:** e1600393

Kim H, Ralph J (2010) Solution-state 2D NMR of ball-milled plant cell wall gels in DMSO-d_6/pyridine-d_5. Org Biomol Chem **8:** 576–591

Kim H, Ralph J, Akiyama T (2008) Solution-state 2D NMR of ball-milled plant cell wall gels in DMSO-d_6. BioEnergy Res **1:** 56–66

Kishimoto T, Uraki Y, Ubukata M (2008a) Synthesis of β-O-4-type artificial lignin polymers and their analysis by NMR spectroscopy. Org Biomol Chem **6:** 2982–2987

Kishimoto T, Uraki Y, Ubukata M (2008b) Synthesis of bromoacetophenone derivatives as starting monomers for β-O-4 type artificial lignin polymers. J Wood Chem Technol **28:** 97–105

Lam TBT, Iiyama K, Stone BA (1992) Cinnamic acid bridges between cell wall polymers in wheat and phalaris internodes. Phytochemistry **31:** 1179–1183

Lu F, Karlen SD, Regner M, Kim H, Ralph SA, Sun R, Kuroda K, Augustin MA, Mawson R, Sabarez H, et al (2015) Naturally *p*-hydroxybenzoylated lignins in palms. BioEnergy Res **8:** 934–952

Lu F, Ralph J (1997) The DFRC method for lignin analysis. Part 1. A new method for β-aryl ether cleavage: lignin model studies. J Agric Food Chem **45:** 4655–4660

Lu F, Ralph J (1999) Detection and determination of *p*-coumaroylated units in lignins. J Agric Food Chem **47:** 1988–1992

Lu F, Ralph J (2002) Preliminary evidence for sinapyl acetate as a lignin monomer in kenaf. J Chem Soc Chem Commun 90–91

Lu F, Ralph J (2003) Non-degradative dissolution and acetylation of ball-milled plant cell walls: high-resolution solution-state NMR. Plant J **35:** 535–544

Lu F, Ralph J (2008) Novel tetrahydrofuran structures derived from β-β-coupling reactions involving sinapyl acetate in kenaf lignins. Org Biomol Chem **6:** 3681–3694

Lu F, Ralph J (2014) The DFRC (derivatization followed by reductive cleavage) method and its applications for lignin characterization. *In* F Lu, ed, Lignin: Structural Analysis, Applications in Biomaterials, and Ecological Significance. Nova Science Publishers, Hauppauge, NY, pp 27–65

Lu F, Ralph J, Morreel K, Messens E, Boerjan W (2004) Preparation and relevance of a cross-coupling product between sinapyl alcohol and sinapyl *p*-hydroxybenzoate. Org Biomol Chem **2:** 2888–2890

Lundquist K, Remmerth S (1975) New synthetic routes to lignin model compounds of arylglycerol-β-aryl ether type. Acta Chem Scand B **29:** 276–278

Mansfield SD, Kim H, Lu F, Ralph J (2012) Whole plant cell wall characterization using solution-state 2D-NMR. Nat Protoc **7:** 1579–1589

Marita JM, Hatfield RD, Rancour DM, Frost KE (2014) Identification and suppression of the *p*-coumaroyl CoA:hydroxycinnamyl alcohol transferase in *Zea mays* L. Plant J **78:** 850–864

Melvin JF, Stewart CM (1969) Chemical composition of the wood of *Gnetum gnemon*. Holzforschung **23:** 51–56

Nakamura Y, Higuchi T (1976) Ester linkage of *p*-coumaric acid in bamboo lignin. Holzforschung **30:** 187–191

Nakamura Y, Higuchi T (1978) Ester linkage of *p*-coumaric acid in bamboo lignin. II. Syntheses of coniferyl *p*-hydroxybenzoate and coniferyl *p*-coumarate as possible precursors of aromatic acid esters in lignin. Cell Chem Technol **12:** 199–208

Pearl IAB, Donald L, Laskowski D (1959) Alkaline hydrolysis of representative palms. Tappi **42:** 779–782

Petrik DL, Karlen SD, Cass CL, Padmakshan D, Lu F, Liu S, Le Bris P, Antelme S, Santoro N, Wilkerson CG, et al (2014) *p*-Coumaroyl-CoA: Monolignol Transferase (PMT) acts specifically in the lignin biosynthetic pathway in *Brachypodium distachyon*. Plant J **77:** 713–726

Ralph J (2010) Hydroxycinnamates in lignification. Phytochem Rev **9:** 65–83

Ralph J, Hatfield RD, Quideau S, Helm RF, Grabber JH, Jung HJG (1994) Pathway of *p*-coumaric acid incorporation into maize lignin as revealed by NMR. J Am Chem Soc **116:** 9448–9456

Ralph J, Lu F (1998) The DFRC method for lignin analysis. Part 6. A modified method to determine acetate regiochemistry on native and isolated lignins. J Agric Food Chem **46:** 4616–4619

Rencoret J, Ralph J, Marques G, Gutiérrez A, Martínez ÁT, del Rio JC (2013) Structural characterization of the lignin from coconut (*Cocos nucifera*) coir fibers. J Agric Food Chem **61:** 2434–2445

Schuetz M, Smith R, Ellis B (2013) Xylem tissue specification, patterning, and differentiation mechanisms. J Exp Bot **64:** 11–31

Sibout R, Le Bris P, Legee F, Cezard L, Renault H, Lapierre C (2016) Structural redesigning *Arabidopsis* lignins into alkali-soluble lignins through the expression of *p*-coumaroyl-CoA:monolignol transferase PMT. Plant Physiol **170:** 1358–1366

Smith DCC (1955a) Ester groups in lignin. Nature **176:** 267–268

Smith DCC (1955b) *p*-Hydroxybenzoates groups in the lignin of aspen (*Populus tremula*). J Chem Soc 2347–2351

Sun RC, Mott L, Bolton J (1998) Isolation and fractional characterization of ball-milled and enzyme lignins from oil palm trunk. J Agric Food Chem **46:** 718–723

Sun RC, Sun XF, Zhang SH (2001) Quantitative determination of hydroxycinnamic acids in wheat, rice, rye, and barley straws, maize stems, oil palm frond fiber, and fast-growing poplar wood. J Agric Food Chem **49:** 5122–5129

Timmel TE (1986) Compression Wood in Gymnosperms. Springer, Heidelberg, Germany

Towers GH, Gibbs RD (1953) Lignin chemistry and the taxonomy of higher plants. Nature **172:** 25–26

Vanholme R, Morreel K, Darrah C, Oyarce P, Grabber JH, Ralph J, Boerjan W (2012) Metabolic engineering of novel lignin in biomass crops. New Phytol **196:** 978–1000

Wagner A, Ralph J, Akiyama T, Flint H, Phillips L, Torr KM, Nanayakkara B, Te Kiri L (2007) Exploring lignification in conifers by silencing hydroxycinnamoyl-CoA:shikimate hydroxycinnamoyltransferase in *Pinus radiata*. Proc Natl Acad Sci USA **104:** 11856–11861

Wilkerson CG, Mansfield SD, Lu F, Withers S, Park JY, Karlen SD, Gonzales-Vigil E, Padmakshan D, Unda F, Rencoret J, et al (2014) Monolignol ferulate transferase introduces chemically labile linkages into the lignin backbone. Science **344:** 90–93

Withers S, Lu F, Kim H, Zhu Y, Ralph J, Wilkerson CG (2012) Identification of a grass-specific enzyme that acylates monolignols with *p*-coumarate. J Biol Chem **287:** 8347–8355